Nanotechnology

Fabrication of nanoscale heterostructure devices with a focused ion beam microscope

Nanotechnology 14 (2003) 630–632 PII: S0957-4484(03)59080-8

Fabrication of nanoscale heterostructure devices with a focused ion beam microscope

C Bell, G Burnell, D-J Kang, R H Hadfield, M J Kappers and M G Blamire

Materials Science Department, IRC in Nanotechnology and IRC in Superconductivity, University of Cambridge, Cambridge, CB2 3QZ, UK

E-mail: cb236@cam.ac.uk

Received 31 January 2003, in final form 19 March 2003
Published 15 April 2003
Online at stacks.iop.org/Nano/14/630

Abstract

A focused ion beam (FIB) microscope has been used to fabricate junctions with dimensions in the range 100–5000 nm by three-dimensional etching. We have applied this process to a variety of structures, including current-perpendicular-to-plane giant-magnetoresistive multilayer devices, superconductor–metal–superconductor Josephson junctions, where the metal is Mo, Co, or a Cu_xNi_{1-x} alloy, and GaN light-emitting diodes. In addition, $Tl_2Ba_2CaCu_2O_8$ intrinsic Josephson junctions were also fabricated and characterized. The flexibility of the FIB technique allowed junctions of many different materials and heterostructures to be fabricated with the same process.

1. Introduction

The methods of device fabrication by lithography and multilevel processing are usually specific to the chemical and physical properties of the etchants and materials used, and require a number of processing steps. For example, a typical device heterostructure requires lithography and chemical or physical milling of a mesa, followed by further lithography for insulation and wiring deposition stages. Each stage requires careful control, and can introduce contamination into the device or the interfaces between layers. As an alternative, the focused ion beam (FIB) microscope is increasingly being used to actively fabricate devices [1]. Kim *et al* [2] have previously used a three-dimensional FIB etching technique to create c-axis Josephson junctions in whiskers and thin films in the high-temperature superconducting cuprates. In this paper we describe our development of this specific technique and its application in creating junctions in a wide range of materials and heterostructures with the FIB, from low-T_C (metallic) superconducting Josephson junctions to semiconducting and magnetic multilayers, as well as intrinsic high-T_C Josephson junctions.

2. Fabrication procedure

The process flow for a typical trilayer film is as follows. The film is grown in a single step (e.g. dc magnetron sputtering for the metallic samples reported in this paper, CVD for semiconducting films, or PLD for oxide materials), which eliminates the problem of interface contamination. The film is patterned with standard optical lithography and broad-beam argon ion milling (500 V, 1 mA cm^{-2}) into a pattern with typically 4 μm wide wires. The remainder of the processing is performed *in situ* in a gallium liquid metal source FIB. The FIB has a spot size of the order of 10 nm with a 4 pA, 30 kV beam. The stage of the FIB can be rotated about an axis collinear with the track in the film between 0° (normal incidence of the beam on the chip) and 45°. Rotation of 180° about an axis normal to the sample stage is also possible. Using a custom-built 45° wedge holder, the two axes of rotation allow the full range of $\theta = 0°–90°$ between the beam and the sample normal to be achieved (see figure 1). To fabricate the device, a section of track typically 5 μm in length was narrowed to around 700 nm with $\theta = 0°$, with a beam current of 150 pA. The sidewalls were then cleaned with a beam current of either 4 or 11 pA and thinned to the final width. This eliminates resputtered material which might otherwise short the device. The sample was then tilted typically to $\theta = 85°$, and the isolating cuts

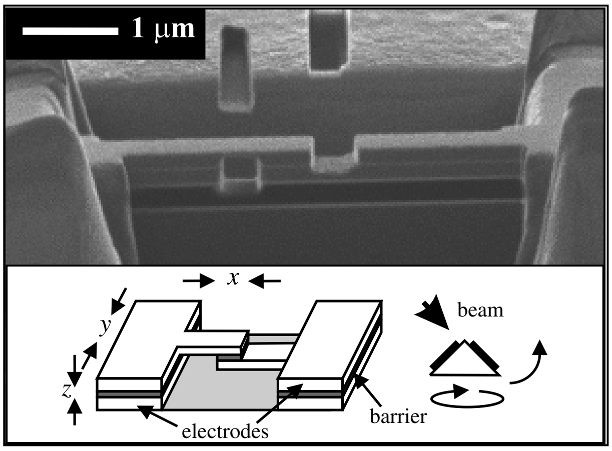

Figure 1. A FIB image of a Nb/CuNi/Nb device viewed from $\theta = 65°$. Inset: a schematic diagram of a generic trilayer device with x-, y-, and z-dimensions (left) and rotation axes on the sample holder.

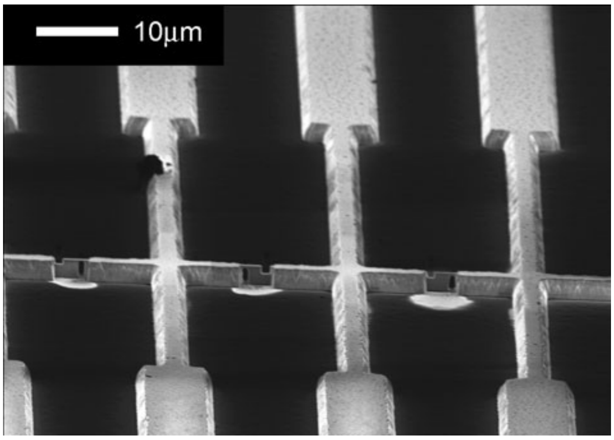

Figure 2. A low-magnification image of several GaN devices from $\theta = 65°$. The main track of the pattern runs left to right, with current/voltage leads running top to bottom.

were made with a beam current of 4 or 11 pA to achieve the final geometry shown in figure 1. In this geometry, current flows horizontally to the base of the included mesa, vertically through the active heterostructure, and out horizontally through the top wiring layer. Figure 2 shows a low-magnification FIB image of the main track of the optically defined pattern (running left to right), along which a series of devices have been fabricated. Current/voltage wires, used for individual electrical measurements, leading to the contact pads run top to bottom.

Device dimensions have been produced in the range $x =$ 200–5000 nm and $y =$ 100–700 nm, with active device region thickness z = 5–250 nm (see figure 1). Since the milling takes place at $\theta = 85°$, rather than 90°, simple trigonometry requires that the isolation cuts must overmill into the electrodes by of the order of 50 nm in the z-direction, to ensure that all the current flows through the barrier. In addition, to allow a margin of error for the spot size/stage drift in the FIB, the electrodes were typically 150 nm or thicker. The y-dimension was constrained by similar trigonometry, so for 150 nm thick electrodes, it could not be larger than 700 nm. We now discuss several examples of this type of process.

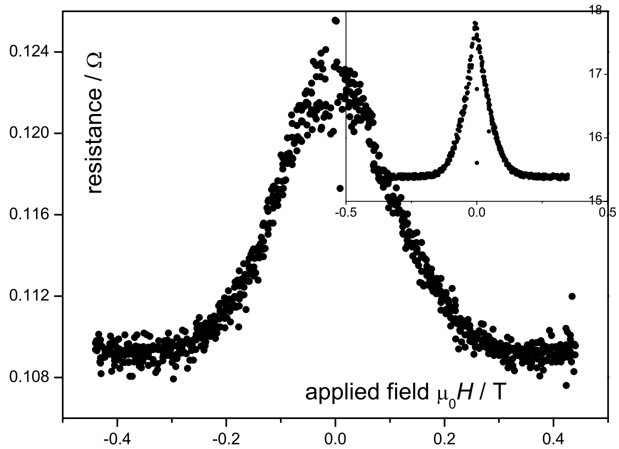

Figure 3. The $R(H)$ curve for CPP GMR sample, with GMR = 14%. Inset: $R(H)$ for the CIP measurement with thin capping Nb layers: GMR = 13%.

3. Results and discussion

Giant magnetoresistance (GMR) is caused by changes in the relative orientation of magnetic layers in a multilayer film, with an applied field H. Current-perpendicular-to-plane (CPP) GMR is of much interest, since the GMR is larger than the equivalent current-in-plane (CIP) measurement and in some respects is easier to analyse. Superconducting electrodes have been used in traditional mesa geometries, with *ex situ* deposited contact wiring, but this requires sensitive measurement due to the low resistance of the devices [3]. Figure 3 shows the CPP GMR of the multilayer Nb(150 nm)[Cu(0.9 nm)Co(2 nm)]$_{10}$Nb(150 nm) (namely $R(H = 0) - R(H = 550\text{ mT})/R(H = 0)$), which is $\sim$14% as measured with superconducting Nb contacts at 0.34 K; the device was of area $\sim$0.8 μm^2, so the resistance change was measurable using conventional electronics. The inset shows the CIP of a nominally identical film, but with only $\sim$4 nm Nb; the CIP GMR is of a similar order. The CPP GMR being smaller than expected is due in part to the increased roughness of the film due to the thicker Nb underlayer needed for the FIB fabrication (this is confirmed by an increased coercive field in the hysteresis loops). Ga damage/implantation has not destroyed the coupling of the multilayer, which can be a problem when using the FIB for nanopatterning magnetic films [4]. We assume that most of the Ga damage caused by the 150 pA beam was removed by the cleaning with a lower beam current; any remaining sidewall damage would be lateral straggle of the order of 10 nm—which may become significant only for the smallest devices studied. Since the side cuts are also made with the lower beam currents, they also introduce minimal damage to the magnetic barrier. Also there are no shunting/superconducting shorts of the barrier caused by resputtered Nb during the processing. This is important for all of the devices that we discuss.

In the case of the superconducting devices, 150 nm thick Nb electrodes are grown above and below the normal metal barrier, of thickness in the range 100–250 nm. The overhanging bridge of Nb typically supported a critical current (I_C) of several milliamperes at 4.2 K; for the devices studied, this is larger than the critical current of the junction. Figure 4

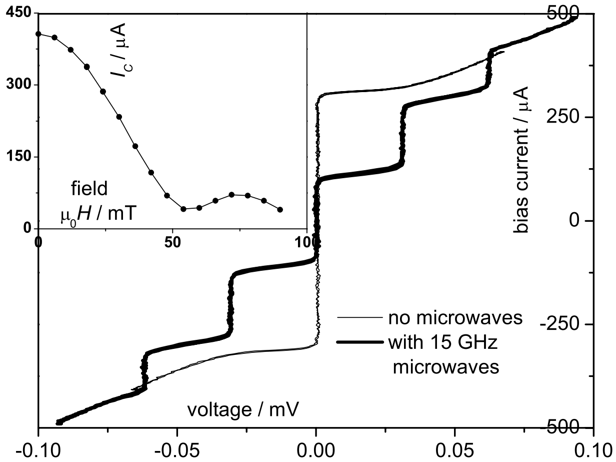

Figure 4. I–V curves for a 0.03 μm^2 area Nb/Mo/Nb junction with and without microwaves. Inset: $I_C(H)$, showing the re-entrant I_C. Lines are a guide to the eye only.

shows the I–V characteristics of a Nb/Mo/Nb junction with $d_{Mo} \sim 180$ nm. The application of microwaves results in Shapiro steps being seen at the expected voltages; the $I_C(H)$ shows re-entrant I_C, indicating the high quality of the junctions. Josephson junctions have also been fabricated in this manner using the ferromagnetic metals Co and Cu_xNi_{1-x} for $x \sim 0.47$ as the barrier, with thicknesses (z) in the range 5–15 nm. This is of particular relevance for the study of ferromagnetic Josephson junctions, which has previously used relatively large junction areas [5, 6]. Using this approach with the FIB, the sub-micron areas approach the order of the magnetic domain size in the barrier layer. New effects may arise due to the non-homogeneous magnetic structure [7]. We have also used the FIB technique to make stacks of hundreds of intrinsic Josephson junctions in c-axis thin films of $Tl_2Ba_2CaCu_2O_8$ [8].

Semiconducting heterostructure devices have also been fabricated. We have created light-emitting diodes using a p-GaN/(GaN/InGaN)$_5$/n-GaN film. Much work has been successfully done with FIB systems to create and improve mirror facets for GaN lasers [9] and also to create HFET pillars [10]. There is interest also in the polarization of devices with high aspect ratio, and dimensions less than or equal to the wavelength of light [11], and also in the scaling of nanoscale diodes [12]. In our geometry, the problems associated with making metal ohmic/low-resistance contacts to p-type GaN [13] are avoided: the p-type layer itself is used as the wiring layer, and no metallization is required. The emitted light can now also escape vertically.

The contrast between the p-type and n-type material is not sufficient to reveal where to make the isolating cuts. If the electrode thicknesses are well known, and the thickness is >200 nm, oversized isolation cuts can be made to overcome this problem. Alternatively, an *in situ* resistance measurement was also used for calibration [14]: peaks appear in the derivative of resistance with respect to time as successive layers are milled through. Cuts from $\theta = 0°$ were thus calibrated to stop at a particular interface, and gave a visible guide when viewed at $\theta = 85°$. Figure 5 shows a FIB image of a GaN device, and, in the insets, an I–V curve and an optical image of the operating diode.

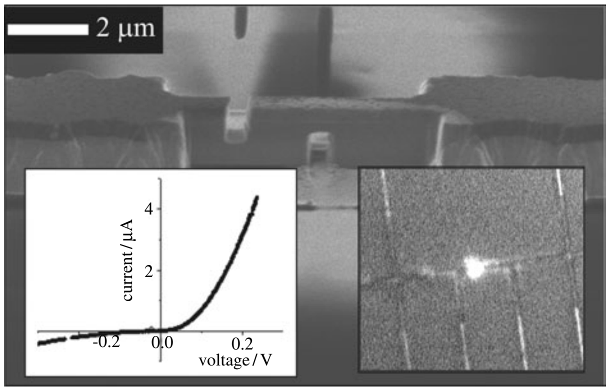

Figure 5. A FIB image from $\theta = 65°$ of a GaN LED. Insets: the I–V characteristic of the device and an optical image of the glowing LED with bias current.

4. Conclusions

In summary, we have fabricated and characterized nanoscale junctions with a simple three-dimensional FIB etching technique. This fabrication technique, which is not material specific, has produced devices with a range of materials and heterostructures.

Acknowledgments

We acknowledge E J Tarte and C W Leung for helpful discussions. This work was supported by the Engineering and Physical Sciences Research Council, UK.

References

[1] Moseley R W, Booij W E, Tarte E J and Blamire M G 1999 *Appl. Phys. Lett.* **75** 262

[2] Kim S-J, Latyshev Yu I and Yamashita T 1999 *Appl. Phys. Lett.* **74** 1156

[3] Pratt W P Jr, Lee S-F, Slaughter J M, Loloee R, Schroeder P A and Bass J 1991 *Phys. Rev. Lett.* **66** 3060

[4] Kaminsky W M, Jones G A C, Patel N K, Booij W E, Blamire M G, Gardiner S M, Xu Y B and Bland J A C 2001 *Appl. Phys. Lett.* **78** 1589

[5] Ryazanov V V, Oboznov V A, Rusanov A Yu, Veretennikov A V, Golubov A A and Aarts J 2001 *Phys. Rev. Lett.* **86** 2427

[6] Kontos T, Aprili M, Lesueur J, Genêt F, Stephanidis B and Boursier R 2002 *Phys. Rev. Lett.* **89** 137007

[7] Bergeret F S, Volkov A F and Efetov K B 2001 *Phys. Rev.* B **64** 134506

[8] Warburton P A, Kuzhakhmetov A R, Bell C, Burnell G, Blamire M G, Wu H, Grovenor C R M and Schneidewind H 2003 *IEEE Trans. Appl. Supercond.* at press

[9] Chyr I, Lee B, Chao L C and Steckl A J 1999 *J. Vac. Sci. Technol.* B **17** 3063

[10] Kuball M, Benyoucef M, Morrissey F H and Foxon C T 2000 *MRS Internet J. Nitride Semicond. Res.* **5S1** W12.3

[11] Hu J, Li L-S, Lang W, Manna L, Wang L-W and Alivisatos A P 2001 *Science* **292** 2060

[12] Smit G D J, Flokstra M G, Rogge S and Klapwijk T M 2002 *Microelectron. Eng.* **64** 429

[13] For example see
Ho J-K, Jong C-S, Chiu C C, Huang C-N, Chen C-Y and Shih K-K 1999 *Appl. Phys. Lett.* **74** 1275 and references therein

[14] Latif A, Booij W E, Durrell J H and Blamire M G 2000 *J. Vac. Sci. Technol.* B **18** 761